Journal of Peptide Science
J. Pept. Sci. 2008; **14**: 518–523
Published online 17 December 2007 in Wiley InterScience (www.interscience.wiley.com). DOI: 10.1002/psc.981

JOURNAL OF PEPTIDE SCIENCE

Structuring and interactions of human β-defensins 2 and 3 with model membranes‡

FRANCESCA MORGERA,[a,b]* NIKOLINKA ANTCHEVA,[b] SABRINA PACOR,[c] LUCA QUARONI,[a] FEDERICO BERTI,[d] LISA VACCARI[a] and ALESSANDRO TOSSI[b]

[a] ELETTRA Synchrotron Light Laboratory, S.S. 14 Km 163.5 in Area Science Park, 34012 Basovizza, Trieste, Italy
[b] Department of Biochemistry, University of Trieste, 34127 Trieste, Italy
[c] Department of Biomedical Sciences, University of Trieste, 34127 Trieste, Italy
[d] Department of Chemical Sciences, University of Trieste, 34127 Trieste, Italy

Received 27 June 2007; *Revised 11 October 2007*; *Accepted 22 October 2007*

Abstract: β-Defensins play an important role in both innate and adaptive immunity, displaying a direct anti-microbial activity against a wide variety of micro-organisms as well as interesting immuno-modulatory effects on host cells. Interaction with biological membranes appears to be a central theme in modulating these activities, leading to different consequences such as membrane lysis, translocation into the cytoplasm or transfer to a receptor. We have investigated the structuring of human β-defensins (hBD2 and hBD3) and rationally designed variants, in relation to their interactions with real and model membranes. Biophysical methods, such as circular dichroism (CD), transmission or reflection IR and dye release were used to probe their structure/activity in the presence of model membranes, while fluorimetric and flow cytometric assays were used to investigate the effects on prokaryotic cells. Our results indicate that structural features, such as the helical *N*-terminal domains and oligomerisation at the membrane surface, may modulate the efficiency of membrane insertion and selectivity for microbial or host-cell membranes. We propose that both peptides interact with membranes as extended β-sheet platforms that present amphipathic helices for insertion into the lipid bilayer. Copyright © 2007 European Peptide Society and John Wiley & Sons, Ltd.

Keywords: anti-microbial peptides; β-defensins; natural immunity; protein-membrane interaction; biological membranes; model membranes

INTRODUCTION

β-Defensins are among the smallest examples of autonomously folding polypeptides, displaying a characteristic fold consisting of a conserved, triple-stranded anti-parallel β-sheet core and a less-conserved *N*-terminal helix of varying stability (Figure 1) [1]. This scaffold depends principally on the presence of six conserved cysteine residues forming three S–S bridges and supports a remarkable sequence variation. Birds and mammals express numerous β-defensins, which are subject to differential evolutionary patterns, ranging from positively selected variation to conservation, consistent with specific adaptations and specialisation within the innate immune response [2,3]. An initial interaction with biological membranes, either microbial or of host cells, is a common and central theme in modulating their activities, although it can subsequently lead to different effects, such as membrane lysis, translocation or transfer to a receptor, depending on the peptide and target. For this reason, we have initiated a systematic study of the structuring and interactions of human β-defensins 2 (hBD2) and β-defensins 3 (hBD3) and rationally designed variants with model membrane systems, correlating these to their effects on bacteria or host cells. Interactions with liposomes or supported lipid multi-layers with specific lipid compositions were probed using transmission and attenuated total reflection (ATR) Fourier transform infrared (FTIR) spectroscopy, CD and fluorescent dye release, while the effect on cells was probed using fluorimetric and flow cytometric methods. On the basis of these results, we are formulating a model for the mode of action at the membrane surface.

MATERIALS AND METHODS

Peptide Synthesis and Characterisation

Fmoc-solid phase peptide synthesis were performed on a PE Biosystems Pioneer peptide synthesis system following the protocol already described previously [2–4].

Preparation of Liposomes

Large unilamellar vesicles (LUVs) were prepared by extrusion of anionic phosphatidyl-DL-glycerol (PG sodium salt from egg yolk lecithin) and cardiolipin (dPG disodium salt from bovine heart), PG/dPG (95 : 5 w/w), or zwitterionic L-α-phosphatidylcholine (PC from egg yolk, Type XVI-E), sphingomyelin (SM from chicken egg yolk) and cholesterol (Ch), PC/SM/Ch (40 : 40 : 20 w/w) dispersions. Lipids were

*Correspondence to: Francesca Morgera, Department of Biochemistry, University of Trieste, 34127 Trieste, Italy;
e-mail: francesca.morgera@elettra.trieste.it
‡ This article is part of the Special Issue of the Journal of Peptide Science entitled "2nd workshop on biophysics of membrane-active peptides".

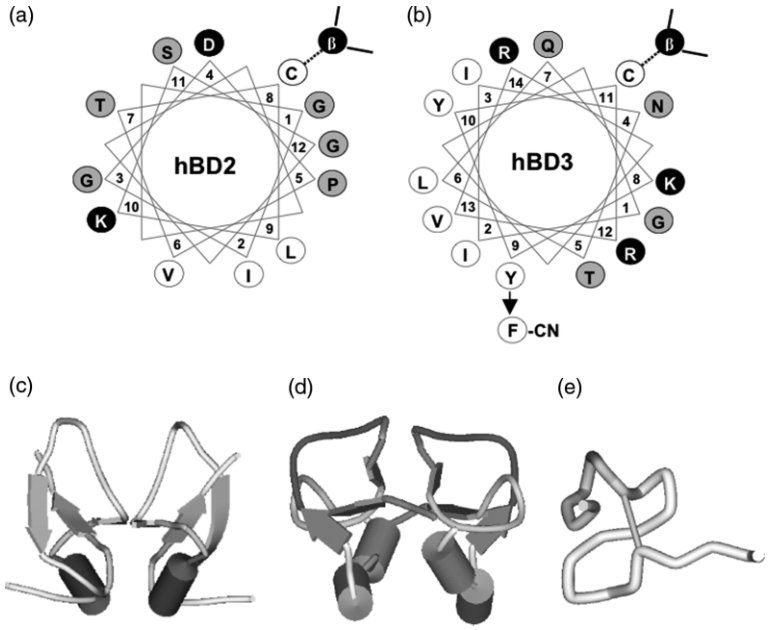

Figure 1 Structural features of hBD2 and hBD3. Helical wheel projections of the *N*-terminal stretches of hBD2 (a) and 3 (b). Neutral hydrophilic residues (grey), charged residues (black) and hydrophobic residues (white) are shown. The cysteine, forming the disulfide bridge with the beta structure is indicated as well; proposed structures of the hBD2 (c) and hBD3 (d) dimers. The former is taken from the crystal structure 1fd3 [8], the latter is modelled on the NMR structure 1KJ6 [9]; modelled structure for *brevi*-hBD2 (e). Construction, docking and minimisations of modelled structures were carried out using the Sybyl 7.0 Tripos packages (to be submitted).

purchased from Sigma Aldrich. Dry lipids were dissolved in chloroform, evaporated under a stream of nitrogen and the residue vacuum-dried for 3 h. The lipid cake was re-suspended to a concentration of 3 mg/ml in the appropriate buffer by spinning the flask at a temperature above the Tc. The resulting multi-lamellar vesicle suspensions were disrupted by several freeze-thaw cycles prior to extrusion with a Mini-Extruder (Avanti Polar Lipids, Inc.) through polycarbonate filters with 100 nm pores.

Circular Dichroism (CD)

CD spectroscopy was performed on a J-715 spectropolarimeter (JASCO Corp. Japan), using 2-mm quartz cells and 20 μM peptide with or without phospholipid vesicles (0.4 mM phospholipids) in 5 mM sodium phosphate buffer (SPB) at pH 7.0 and room temperature. The peptide–lipid suspensions (molar ratio 1 : 20) were incubated for 30 min. at 37 °C before use. The spectra are the average for at least two independent experiments, each with accumulation of three scans.

ATR-FTIR

Spectra were collected with the HORIZON multiple reflectance ATR accessory (Harrick Scientific Products, Inc.) mounted on a Bruker Vertex 70 FTIR spectrometer equipped with a Mid Band Mercury-Cadmium-Telluride detector (MCT D316), by acquiring 256 scans with a resolution of 4 cm^{-1}. The background was collected directly on a clean internal reflection element (IRE). The peptide (20 μM) was incubated with phospholipid vesicles (0.4 mM phospholipids) in 5 mM SPB at pH 7.0, further deposited on a Ge trapezoidal 45° ATR crystal (50 mm × 10 mm × 2 mm) at 37 °C. The buffer evaporation resulted in lipid multi-layers on which the spectrum was recorded [5]. Any contribution of water vapour to the absorbance spectra on the amide I peak region was corrected by spectral subtraction.

Transmission FTIR

Spectra (512 scans, spectral resolution 2 cm^{-1}) were collected with Vertex 70 Bruker interferometer, using 2 mM peptide solutions in D_2O placed between CaF_2 windows, spaced 25 microns apart in a dismountable liquid cell (Harrick Scientific Products, Inc.), after allowing the amide II band to shift from 1550 to 1460 cm^{-1} to ensure complete deuterium exchange. Non-linear least-square curve fitting with Gaussians bands was used to identify the components of the amide I band. Starting parameters for the fitting process were obtained by second-derivative spectra (9-data-point Savitzky-Golay algorithm).

Microbiological Assays

The anti-microbial activity of the synthetic peptides was determined as the MIC using the micro-dilution susceptibility test, and the killing kinetics by plating after exposure to peptides for increasing times, as described previously [2–4]. The permeabilisation of the cytoplasmic membrane of *E.coli* by the peptides was evaluated by following hydrolysis of an impermeant substrate by a cytoplasmic hydrolase [2–4].

Flow Cytometric Assays

Permeabilisation of single *E.coli* cells was evaluated by following propidium iodine (PI) fluorescence with a Cytomics

DOI: 10.1002/psc

FC 5000 (Beckman Coulter, Inc., Fullerton, CA), equipped with an Argon laser (488 nm, 5 mW), and supported by forward and side light scatter detectors and five PMT fluorescence detectors. Suspensions of 10^6 *E.coli* ML35 in 5% Triptic Soy Broth dissolved in SPB were exposed to 1 μM of the desired peptide, and after 1 min of incubation with PI (10 μg/ml) at 37 °C, PI fluorescence was followed for 40 min.

RESULTS AND DISCUSSION

Peptide Structure and Structure Prediction

Here hBD2 and 3 both conform to the canonical β-defensin β-sheet scaffold [1], but have quite different sequences apart from conserved cysteines and *N*-terminal domains. We have chemically synthesised rationally designed variants of both peptides to probe the roles of different structural elements in mediating membrane interactions (Table 1).

Thus, hBD2 displays a stable, mildly amphipathic, *N*-terminal helix (Figure 1(a)) [6] and is mostly monomeric in bulk solution, but may become dimeric via formation of an extended β-structure at higher concentrations, such as those at the membrane surface [6–8]. The helix is stabilised by a key Asp residue (D^4), involved in a number of intra-molecular interactions, which was deleted in (−D)hBD2, while the truncated peptide (5–41) hBD2 is entirely devoid of this structural element [7]. In *brevi*-hBD2 the helical domain is maintained while removing most of the β-sheet platform. It has been modelled to show that a helix could still form, stacked on a β-hairpin (Figure 1(e)).

hBD3 is reported to have a dimeric/oligomeric structure [4,9], which is proposed to occur via electrostatic interactions [9] without requiring an extended β-structure. Its *N*-terminal stretch shows a less defined conformation in solution [9], but if a helix were to form it would be quite amphipathic (Figure 1(b)) and would thus be favoured by contact with membranes. A chimeric peptide [(1–8)hBD2(12–45)hBD3] was synthesised in which the stable hBD2 helix was grafted onto the highly cationic hBD3 β-sheet core. Finally, in CN-hBD3, Tyr^9 at the centre of its putative amphipathic *N*-terminal helix (Figure 1(b)) was replaced with an isosteric *p*-cyanophenylalanine residue to act as an IR environmental probe. Models of hBD2 and hBD3 dimers with completely structured *N*-terminal domains indicate they would both present anti-parallel amphipathic helices below an extended β-sheet platform (Figure 1(c), (d)). These helices might serve to direct the above-lying platforms into the membranes, but otherwise the mechanism of action may be quite different from that of linear helical AMPs. Moreover, the presence of the helical stretch does not seem to be strictly essential for anti-microbial activity.

Probing Structures by CD and FTIR

Secondary structure variations were investigated by CD at low peptide concentration (20 μM) in phosphate buffer, trifluoroethanol (TFE) and membrane-like systems (SDS micelles and liposomes) (Figures 2–3). Liposomes, with appropriate anionic or zwitterionic phospholipids compositions, were respectively used to model interaction with bacterial and host-cell membranes.

CD spectra for hBD2 (Figure 2(a)) were dominated by a single maximum (196 nm) and a minimum (218 nm) with a shoulder at 222 nm, consistent with a stable β-sheet nucleus and a helical segment [10]. This conformation is evident in all tested environments and is in agreement with a helical content of about 10%, in line with NMR and X-ray structures, showing about 5 out of 41 helical residues in a helical conformation [6–8]. For (−D)hBD2 and (5–41)hBD2 (Figure 3(a) and (b)), there is no evidence of a helical conformation in an aqueous environment, which also seemed to cause a reduction of β-sheet content, although for (−D)hBD2 a recovery of both helix and β-sheet conformations was apparent in a membrane-like

Table 1 Sequence of synthesised β-defensin peptides and analogues: chemical properties and qualitative data of bacterial inactivation on *E.coli* and *S.aureus* are reported

Peptide	Sequence	MW (Da)	Charge	Bacterial[a] Inactivation	
				E.c.	S.a.
hBD2	GIGDPVT**C**LKSGAI**C**HPVF**C**PRRYKQIGT**C**GLPGTK**CC**KKP	4328	6	+++	++
(−D)hBD2	GIG-PVT**C**LKSGAI**C**HPVF**C**PRRYKQIGT**C**GLPGTK**CC**KKP	4213	7	+++	++
(5–41)hBD2	----PVT**C**LKSGAI**C**HPVF**C**PRRYKQIGT**C**GLPGTK**CC**KKP	3986	7	++	+
Brevi hBD2	GIGDPVT**C**LKS----------GLPGTK**C**ARRKKP	2483	5	−	−
hBD3	GIINTLQKYY**C**RVRGGR**C**AVLS**C**LPKEEQIGK**C**STRGRK**CC**RRKK	5155	11	++++	++++
hBD3-CN	GIINTLQKFY**C**RVRGGR**C**AVLS**C**LPKEEQIGK**C**STRGRK**CC**RRKK	5169	11	/	/
hBD2/3chimera	GIGDPVT**C**RVRGGR**C**AVLS**C**LPKEEQIGK**C**STRGRK**CC**RRKK	4600	10	++++	++++

[a] based on MIC values F = p-cyanophenylalanine.

DOI: 10.1002/psc

environment. The spectrum of *brevi*-hBD2 (Figure 3(c)) indicated a prevalently random coil conformation (negative band at 190 nm) but also underwent a transition to a partly helical structure in SDS micelles and TFE. hBD3 was less structured than hBD2 in an aqueous solution but, as predicted, showed a marked coil-helix transition in the presence of anionic LUVs (Figure 2(b)) as well as SDS (data not shown).

The attenuated total reflectance (ATR)-FTIR was used to further probe the interaction of CN-hBD3 with model membranes (Figure 2(c)), by monitoring the cyano-stretching mode in the cyano-Phe[9] strategically placed in the centre of the amphipathic helix polar sector (Figure 1(b)). The strong shift of the CN group band, from 2235 cm^{-1} in buffer to 2229 cm^{-1} in lipids, is compatible with the insertion of a helical segment into the membrane [11]. CD and ATR-FTIR experiments thus indicate that membrane interaction induces helical structuring of the amphipathic *N*-terminal stretch, which may then partly insert into the bilayer.

The structural characteristics of hBD2 and 3, and in particular their aggregation, was also studied by FTIR transmission spectroscopy of 2mM peptide solutions in D_2O (Figure 4, Table 2). FTIR spectra confirmed CD results, although the former underestimates helix content and better evidences beta structures [12], contrary to the CD technique. FTIR further highlighted the presence of aggregated β-structures, according to the component assignments showed in Table 2 [13]. In Figure 4(a) and (b), hBD2 shows a narrower band than its variants or hBD3, with well defined shoulders at positions consistent with a stable β-structure and possible β-aggregation, via β-sheet interaction, which is compatible with the high concentration required for transmission experiments, and is in agreement with the formation of dimers within oligomers as observed by X-ray diffraction [8].

The (−D) and (5–41) hBD2 analogues show broader bands, consistent with a more random structure, as well as a less stable or absent helical segment. (−D)hBD2 seems the more structured of the two and may present some β-aggregation, while the complete absence of the *N*-terminal stretch may compromise the stability of the entire molecule. Brevi-hBD2 is the least structured peptide with no evidence for β-aggregation (Figure 4(a), Table 2).

hBD3 and the hBD2/3 chimera (Figure 4(b), Table 2) also give rise to broader IR bands, which evidence a higher proportion of random coil than hBD2, confirming CD results in aqueous solution. Spectra are also characterised by the two typical components assigned to the symmetric and anti-symmetric stretching of deuterated arginine side chains (1608 and 1585 cm^{-1} respectively), of which they are very abundant (16–17%

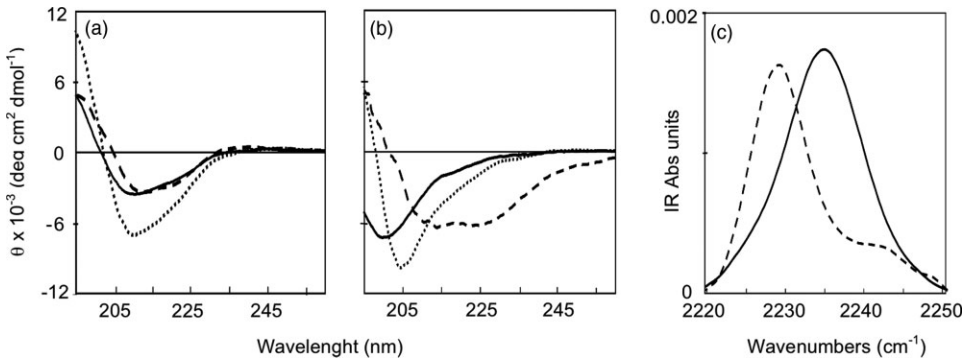

Figure 2 CD and IR spectra of hBD2 and hBD3. CD spectra of hBD2 (a) and hBD3 (b) [20 μM peptide; 0.4 mM lipids in SPB] and IR spectrum of CN stretching of hBD3-CN (c) [2mM peptide in water, 20 μM peptide in 0.4 mM lipids in SPB]. SPB [10mM pH 7.0] (———); anionic PG/dPG LUVs (- - - -); zwitterionic PC/SM/Ch LUVs (·····).

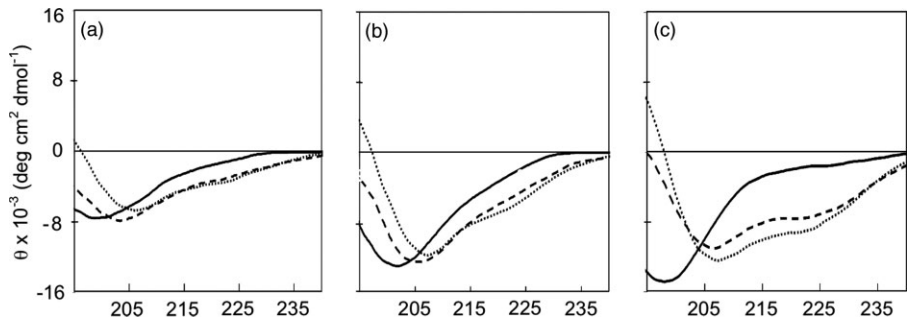

Figure 3 CD spectra of hBD2 analogues. CD spectra of (−D)hBD2 (a), (5–41)hBD2 (b), *brevi*-hBD2 (c) [20 μM peptide]. SPB buffer (———); SDS micelles (- - - -) [10mM SDS in SPB]; TFE (·····) [50% TFE in SPB].

DOI: 10.1002/psc

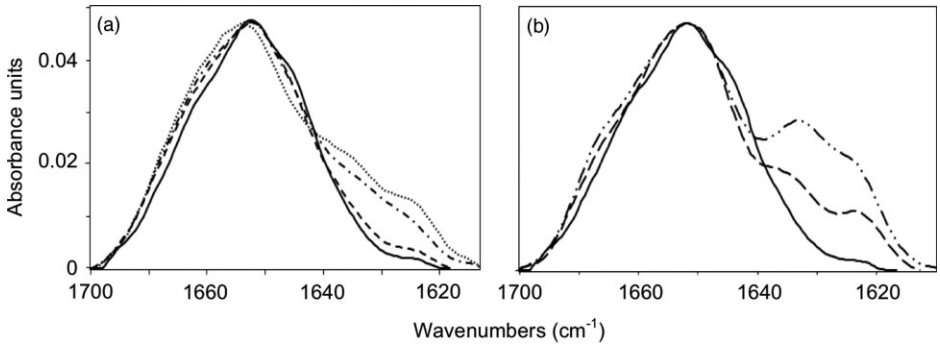

Figure 4 FTIR transmission spectra of β-defensins in deuterated water, amide I band. FTIR spectra of hBD2 (———), (−D)hBD2 (- - - -), (5–41)hBD2 (– · – · – ·) and *brevi* hBD2 (· · · · · ·) (a) and hBD2 (———), hBD3 (- - - -), hBD2/3 chimera (– · · – · ·) (b) [2 mM peptide in D_2O, after complete H/D exchange].

Table 2 FTIR secondary structure assignments: assignment of secondary structure elements determined by curve fitting of the deuterated amide I band of human peptides (wavenumbers (ν) and relative areas). Peak assignment for aggregated structure [Byler and Susi, 1984 (*)] and AA side chain Arg are also reported

Peptide	β-Structure		α-Helix		Turns/loop		Random coil		Aggregated structure*	AA side chain Arg
	ν (cm^{-1})	Area (%)	ν (cm^{-1})	Area (%)	ν (cm^{-1})	Area (%)	ν (cm^{-1})	Area (%)	ν (cm^{-1})	ν (cm^{-1})
hBD2	1628	32	1651	5	1662	22	1644	41	1612	
	1672								1680	
(−D)hBD2	1628	33	—	—	1660	21	1643	45	1613	
	1670								1681	
(5–41)hBD2	1623	33	—	—	1659	21	1642	45		
	1673									
Brevi-hBD2	1625	25	—	—	1661	20	1643	55		
	1674									
hBD3	1624	24	1653	4	1661	11	1641	60		1585 (ν_a)
	1673									1607 (ν_s)
hBD2/3 chimera	1623	26	1654	6	1663	8	1641	60		1585 (ν_a)
	1673									1607 (ν_s)

of all residues). In this case, the absence of significant β-aggregation components may be consistent with the fact that oligomerisation occurs via salt-bridging rather than β-sheet interaction [4].

Biological Activities

The anti-microbial potency of the β-defensin variants, qualitatively shown in Table 1, is based on MIC evaluations against a reference Gram-negative and Gram-positive strain (respectively *E. coli* ML-35 and *S. aureus* 710A, to be submitted). In general, these data correlate with cationicity, as hBD3 and the hBD2/3 chimera are the most active. For hBD2 and its analogues, the presence or absence of the *N*-terminal helical segment seemed to have little effect on bacterial inactivation, while that of the β-sheet core appeared to be essential. The effect of peptides on bacterial membranes was probed for *E.coli* ML-35, by following internalisation of the fluorescent probe PI and the chromogenic hydrolase substrate o-Nitrophenyl-beta-D-galactopyranosid (ONPG), in order to better understand the kinetics of membrane damage (Figure 5(a), (b)). Flow cytometric assays revealed that the cationic PI is internalised rapidly (Figure 5(a)) and its internalisation is followed by morphological changes in bacterial cells after 30 min exposure to the peptides, as judged by variation in forward and side scatter (data not shown). The highly cationic hBD3 seems to be more efficient in inducing these effects than hBD2. The killing kinetics were also more rapid for hBD3 than hBD2 (Figure 5(c)). Permeabilisation to the neutral ONPG, induced by either these peptides or the (−D)hBD2 variant, was slower, becoming significant only after a considerable lag-time (30 min; Figure 5(b)). Taken together, these results may indicate a rapid compromising of the membrane, which is favoured by the higher cationicity of hBD3, and which

DOI: 10.1002/psc

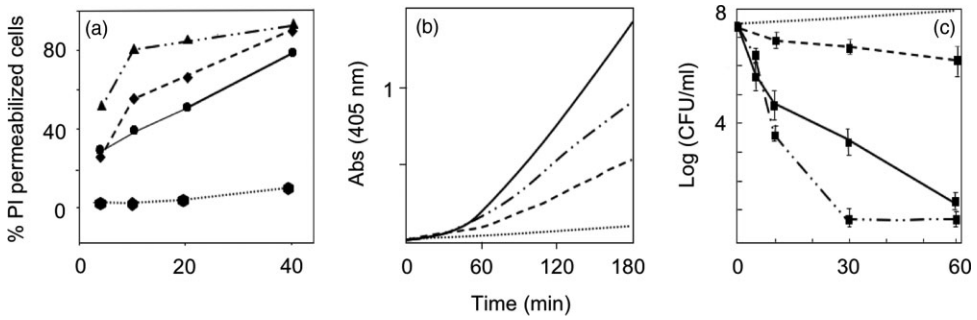

Figure 5 Bacterial membrane permeabilisation kinetics. Flow cytometry analysis of *E.coli* ML-35 permeabilisation to propidium iodide (1 μM peptide, 10^6 CFU/ml *E.coli* ML35) (a); ONPG colorimetric assay (10 μM peptide, 10^7 CFU/ml *E.coli* ML35/pYC) (b); bacterial killing kinetics (8 μM peptide, 10^7 CFU/ml *E.coli* ML35) (c). Control (·····), hBD2 (———), (–D)hBD2 (- - - -), hBD3 (– ··– ··).

initiates an irreversible killing process, but which may not be the primary killing effect. A subsequent slower alteration of the bacteria may result in a later, more massive damage to the membrane.

CONCLUSIONS

Our results suggest that both hBD2 and 3 may interact with membranes as cationic β-sheet platforms, presenting amphipathic helices for insertion into the lipid bilayer. This helix is pre-formed in hBD2, whereas membrane-stabilised in hBD3. Its presence seems to modulate the anti-microbial activity but not be strictly necessary for it (see bacterial inactivation in Table 1). The β-sheet platform appears to be the primary structural element required for anti-microbial activity, while the helical stretch may modulate it, affecting membrane selectivity and/or killing kinetics. Both peptides may act as dimeric (or oligomeric) platforms, forming in solution or at the membrane surface, that present aligned, anti-parallel helices to the membrane for insertion. Interaction of the peptides with the membrane then leads to its permeabilisation, which may proceed in stages and only be the initial phase of the killing mechanism.

Ongoing experiments are probing the mechanisms of membrane interaction and permeabilisation of hBD2 and 3. In particular, we aim to verify if the presence of a pre-formed helix in hBD2 favours its interaction with host-cell membranes, possibly explaining its remarkable immuno-modulating properties, and if the membrane-induced helix in hBD3 affects its selectivity for bacterial membranes.

Acknowledgements

We gratefully acknowledge Prof. Giacinto Scoles for supporting the purchase of the HORIZON unit.

This work was supported by FVG Region project no. 200502027001.

REFERENCES

1. Pazgier M, Hoover DM, Yang D, Lu W, Lubkowski J. Human beta-defensins. *Cell. Mol. Life. Sci.* 2006; **63**: 1294–1313.
2. Crovella S, Antcheva N, Zelezetsky I, Boniotto M, Pacor S, Verga Falzacappa MV, Tossi A. Primate beta-defensins: structure, function and evolution. *Curr. Protein Pept. Sci.* 2005; **6**: 7–21.
3. Antcheva N, Boniotto M, Zelezetsky I, Pacor S, Verga Falzacappa MV, Crivella S, Tossi A. Effects of positively selected sequence variations in human and macaca fascicularis β-defensins 2 on antimicrobial activity. *Antimicrob. Agents Chemother.* 2004; **48**: 685–688.
4. Boniotto M, Antcheva N, Zelezetsky I, Tossi A, Palumbo V, Verga Falzacappa MV, Sgubin S, Braida L, Amoroso A, Crovella S. A study of host defence peptide beta-defensin 3 in primates. *Biochem. J.* 2003; **374**: 707–714.
5. Silvestro L, Axelsen PH. Infrared spectroscopy of supported lipid monolayer, bilayer, and multibilayer membranes. *Chem. Phys. Lipids* 1998; **96**: 69–80.
6. Sawai MV, Jia HP, Liu L, Aseyev V, Wiencek JM, McCray PB Jr, Ganz T, Kearney WR, Tack BF. The NMR structure of human beta-defensin-2 reveals a novel alpha-helical segment. *Biochemistry* 2001; **40**: 3810–3816.
7. Bauer F, Schweimer K, Kluver E, Conejo-Garcia JR, Forssmann WG, Rosch P, Adermann K, Sticht H. Structure determination of human and murine beta-defensins reveals structural conservation in the absence of significant sequence similarity. *Protein Sci.* 2001; **10**: 2470–2479.
8. Hoover DM, Rajashankar KR, Blumenthal R, Puri A, Oppenheim JJ, Chertov O, Lubkowski J. The structure of human beta-defensin-2 shows evidence of higher order oligomerization. *J. Biol. Chem.* 2000; **275**: 32911–32918.
9. Schibli DJ, Hunter HN, Aseyev V, Starner TD, Wiencek JM, McCray PB, Tack BF, Vogel HJ Jr. The solution structures of the human beta-defensins lead to a better understanding of the potent bactericidal activity of HBD3 against Staphylococcus aureus. *J. Biol. Chem.* 2002; **277**: 8279–8289.
10. Fasman GD. *Circular Dichroism and the Conformational Analysis of Biomolecules*. Plenum Press: New York, 1996; 69–158.
11. Tucker MJ, Getahun Z, Nanda V, DeGrado WF, Gai F. A new method for determining the local environment and orientation of individual side chains of membrane-binding peptides. *J. Am. Chem. Soc.* 2004; **126**(16): 5078–5079.
12. Pribić R, van Stokkum IH, Chapman D, Haris PI, Bloemendal M. Protein secondary structure from Fourier transform infrared and/or circular dichroism spectra. *Anal. Biochem.* 1993; **214**(2): 366–378.
13. Byler DM, Susi H. Examination of the secondary structure of proteins by deconvolved FTIR spectra. *Biopolymers* 1986; **25**: 469–487.